CrossMark
click for updates

Complexation of Eu(III) with Cucurbit[n]uril, n = 5 and 7: A Thermodynamic and Structural Study†

Neetika Rawat,*[a] Aishwarya Kar,[a] A. Bhattacharyya,[b] Ankita Rao,[a] S. K. Nayak,[c] C. Nayak,[d] S. N. Jha,[d] D. Bhattacharyya[d] and B. S. Tomar[a]

Cucurbit[n]urils (CBn) are a new class of macrocyclic cage compounds capable of binding organic and inorganic species, owing to their unique pumpkin like structure comprising of both a hydrophobic cavity and a hydrophilic portal. The thermodynamics of the complexation of Eu(III) with CBn of a different cavity size viz. cucurbit[5]uril (CB5) and cucurbit[7]uril (CB7) has been studied by UV-Vis spectroscopy and calorimetry at 25 °C whereas the structure of the complexes was investigated using time resolved fluorescence spectroscopy (TRFS) and extended X-ray absorption fine structure spectroscopy (EXAFS) in a formic acid–water mixture (50 wt%). This is the first report on the structural investigation of Eu–CBn complexes in solution. The thermodynamic data (ΔG, ΔH and ΔS) for Eu(III) complexation with CBn reveal the formation of a 1 : 1 complex with CB5, while both 1 : 1 and 1 : 2 complexes are observed with CB7. The signatures of these species are observed in ESI-MS measurements, which corroborates with the species postulated in thermodynamic studies. The complexation reactions are found to be driven by ΔS as ΔH is either small negative or positive indicating the formation of inner sphere complexes, which is in line with TRFS and EXAFS results. These studies show that Eu(III) caps one of the CB5 portals by binding with all the carbonyl groups in the 1 : 1 Eu–CB5 complex, whereas in the 1 : 1 Eu–CB7 complex, Eu(III) interacts with only a few of the carbonyl groups of CB7. The computational studies (DFT calculations) on Eu–CB5 and Eu–CB7 complexes further support the experimental data.

Introduction

The study on host–guest interactions with macrocyclic ligands like cyclodextrin, calixarenes, and cucurbituril has been an area of great research interest.[1–4] The inclusion of guest molecules into complementary host structures has been used to engineer the intrinsic molecular properties of guest molecules for desired applications. These molecules mimic important biological ligands, enhance various photophysical spectroscopic properties, catalyze processes, and alter the reactivity of guest species. These ligands impart a unique stability to the guest moiety through various non-covalent interactions. The molecular organization of these ligands with respect to guest moieties maximizes their interaction and thus provides a unique specificity towards guest species.[5] Cucurbit[n]urils (CBn), where n = number of glycolurils, are one of the promising macrocyclic ligands which are formed by the acid catalyzed condensation of glycoluril and formaldehyde and have a high affinity for various organic and inorganic species (Fig. 1).

CBn have a hydrophobic cavity (dia. 4–9 Å) depending on the glycoluril units and a height of 9.1 Å. The presence of the hydrophobic cavity is responsible for their binding with organic guest molecules.[6–8] At both the portals of CBn, carbonyl groups are located pointing towards the centre of the portal. These carbonyl groups are responsible for binding to
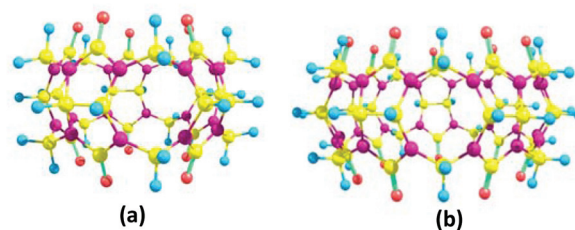
[a]Radioanalytical Chemistry Division, Bhabha Atomic Research Centre, Mumbai – 4000 085, India. E-mail: neetika@barc.gov.in
[b]Radiochemistry Division, Bhabha Atomic Research Centre, Mumbai – 4000 085, India
[c]Bioorganic Chemistry Division, Bhabha Atomic Research Centre, Mumbai – 4000 085, India
[d]Atomic and Molecular Physics Division, Bhabha Atomic Research Centre, Mumbai – 4000 085, India
†Electronic supplementary information (ESI) available: ESI-MS spectra, optimised geometries free CB5, CB7 and their Eu(III) complexes. See DOI: 10.1039/c4dt03623a

Fig. 1 Structure of (a) CB5 and (b) CB7 (Oxygen atom (red), Hydrogen atom (blue), Nitrogen atom (purple), Carbon atom (yellow)).

ionic species through ion dipole interactions. The binding of CBn towards guest molecules has been studied by various techniques *viz.* UV-Vis spectroscopy, ^{1}H-NMR spectroscopy and isothermal calorimetry.[6] A binding constant as high as 3×10^{15} M^{-1} has been observed for CB7 interaction with a ferrocene derivative.[9] In the case of metal–CBn complexes, a large number of crystal structures have been reported with various alkali, alkaline earth, transition metals, lanthanide and actinide ions.[10–12] In the solid state, some of the metal ions were found to interact with only a fraction of the carbonyl oxygen atoms of CBn portals. However, transition metal ions do not interact directly but through water molecules coordinated to metal ions.[13–15] In recent years, many fascinating crystal structures have been reported by introducing small organic molecules as "structure inducers" in metal CBn complexes.[16–19] In most of the cases, complexation of Ln^{3+} to both the portals of CBn molecules has led to the formation of coordination polymers or two dimensional networks. The binding of metal ions with CBn in solution is less clearly understood due to their low solubility in most of the common solvents. Most of the studies in solution are aimed at understanding the mechanism of binding between alkyl ammonium salts and neutral guest molecules.[3,20–22] But complete studies on the thermodynamic and structural parameters for the binding of CBn with metal ions in solution are scarce. Zhang *et al.* determined the thermodynamic data for the complexation of decamethyl cucurbit[5]-uril (MeCB5) with alkali, alkaline earth metals, Pb^{2+} and Cd^{2+}.[23] The authors observed a very high selectivity of MeCB5 for Pb^{2+}. The order of the stability constant for the binding of MeCB5 with alkali and alkaline earth metals was K$^+$ > NH$_4^+$ > Rb$^+$ > Li$^+$ > Cs$^+$ and Sr^{2+} > Ba^{2+} > Ca^{2+} > Mg^{2+} respectively.

So far, a study on the complexation of lanthanide ions with CB5 and CB7 in solution has not been reported in the literature and the studies with CB6 are also limited to the determination of thermodynamic parameters using calorimetry.[24] To the best of our knowledge, this is the first report on the structural investigation of CBn (n = 5 and 7) complexes with lanthanides in solution. The molecular structure of complexes in solution provides indepth information about the binding mechanism which in turn helps in designing more efficient host molecules. Time resolved fluorescence spectroscopy (TRFS) and extended X-ray absorption fine structure spectroscopy (EXAFS) are powerful tools for probing the structure of the host–guest complex at the molecular level in solutions. The fluorescence spectra give information about the electronic environment around the metal ion and in some cases (*viz.* Eu(III)) the number of water molecules in its inner coordination sphere can be determined from the fluorescence lifetime. EXAFS has been extensively used to determine the number and type of atoms present around the probe atom and their distances.[25] A systematic study on the complexation of Eu(III) with CB5 and CB7 has been carried out in a formic acid (FAH)–water (50 wt%) medium with the aim to understand the species and structure of the complexes in solution. The stability constant and enthalpy of complexation were determined by UV-Vis spectroscopy and calorimetry and the stoichiometry

of complexes obtained from thermodynamic studies was also supported by electron spray ionization–mass spectrometry (ESI-MS) measurements. The coordination of Eu(III) on binding with CBn molecules of different cavity sizes *viz.* n = 5 and 7 was investigated by EXAFS and TRFS.

Experimental

Reagents and chemicals

Formic acid and nitric acid used in the present work were of A. R. grade and MilliQ water (18 MΩ cm) was used to prepare all solutions. CB5 and CB7 used in the present work were synthesized following the procedure described below.

Experimental procedure for the syntheses of CB5 and CB7

Both CB5 and CB7 were prepared following a reported procedure[26]: to a suspension of glycoluril (11.4 g, 80.0 mmol) and formaldehyde (37% in water, 14 ml, 172 mmol) at 0–5 °C was added 9 M H$_2$SO$_4$ (40 ml). The solid suspension was heated at 75 °C for 24 h and then further heated at 100 °C for 12 h under stirring. The reaction mixture was cooled to ambient temperature and poured into 400 ml of water. Acetone (2 L) was then added to the mixture to obtain a white precipitate. The mixture was allowed to stand for 15 min, filtered and the residue was washed with a 1 : 4 mixture of water–acetone (2 L) twice. The resulting solid was suspended in a 1 : 1 mixture of water–acetone (400 ml) and stirred for 15 min. The mixture was filtered and the residue was washed with water (200 ml). Acetone (1.5 L) was added to the filtrate to produce a precipitate which was filtered, washed with acetone and dried under vacuum to obtain a colourless solid (a mixture of CB5 and CB7). The solid was further dissolved in water (150 ml) and then methanol was added slowly till precipitation started. The mixture was kept overnight and filtered, washed with methanol and dried under vacuum to yield pure CB7 (0.660 g, 5.0%). To the filtrate acetone was added to precipitate CB5, filtered, washed with acetone and dried to yield pure CB5 (0.300 g, 2.3%). Both CB5 and CB7 were characterized by ^{1}H NMR, ^{13}C NMR and mass spectral (MALDI-TOF) data and matched with those of authentic samples.

Preparation of Eu(III) stock solution

Eu$_2$O$_3$ (Merck, purity > 99.99%) was dissolved in nitric acid which was evaporated to dryness and 0.1 M HNO$_3$ was added to the solid residue. The concentration of Eu(III) was standardized by complexometric titration with EDTA using xylenol orange as the indicator. The Eu(III) in nitric acid was evaporated to dryness and an FAH–water mixture (50 wt%) was added to obtain the desired Eu(III) concentration.

Uv-Vis spectroscopy

Uv-Vis spectrophotometric measurements were carried out using a JASCO-630 spectrophotometer. The change in the absorption spectra of CB5 and CB7 in the range 260–330 nm was measured at a scan rate of 200 nm s^{-1}. 2.0 ml of CB5

(9.69 × 10^{-4} M) or CB7 (1.28 × 10^{-3} M) in an FAH–water mixture was taken in a cuvette and titrated with Eu(III) in the same medium till the Eu(III) concentration was nearly 3 times excess that of CBn. The absorbance ($A^i(\lambda)$) at a particular wavelength (λ) for the ith injection can be related to the free concentrations of different absorbing species (X_j^i is the concentration of the jth species at the ith injection) using the Lambert Beer's law:

$$A^i(\lambda) = l \sum \varepsilon_j(\lambda) X_j^i \qquad (1)$$

where $\varepsilon_j(\lambda)$ is the molar extinction coefficient of the jth species. The matrix $A(N, \Lambda)$ for N titration points and Λ spectral points is solved in conjunction with the mass balance equations (3) and (4) for the total metal ion and ligand concentrations respectively to obtain the free concentrations of the species and thereby the equilibrium constant, using Hyperquad 2006.[27]

$$x\mathrm{M} + y[\mathrm{L}] = \mathrm{M}_x\mathrm{L}_y \qquad (2)$$

$$C_{\mathrm{Mi}}^{\mathrm{T}} = \left[[\mathrm{M}]_i + \sum x\beta_{xy}[\mathrm{M}]_i^x[\mathrm{L}]_i^y \right] \qquad (3)$$

$$C_{\mathrm{Li}}^{\mathrm{T}} = \left[[\mathrm{L}]_i + \sum y\beta_{xy}[\mathrm{M}]_i^x[\mathrm{L}]_i^y \right] \qquad (4)$$

where $C_{\mathrm{Mi}}^{\mathrm{T}}$ and $C_{\mathrm{Li}}^{\mathrm{T}}$ are the total concentrations of metal ions and ligands respectively and $[\mathrm{M}]_i$ and $[\mathrm{L}]_i$ are their equilibrium concentrations at the ith injection. Different possible sets of species ($x = 1$–2 and $y = 1$–3) were given as the input but the software was converged with a specific set of species to give the lowest χ^2.

Calorimetry

Calorimetric experiments were conducted with an isothermal titration calorimeter system (Nanocalorimeter TAM-III, Thermometric AB, Sweden). It is a twin thermopile heat conduction type calorimeter and the differential power signal measured is dynamically corrected for the thermal inertia of the system. Details of the instrument are given elsewhere.[28,29] Before each experiment the instrument was calibrated electrically and the performance of the instrument was tested by measuring $\log K$ and ΔH for the reaction between $\mathrm{BaCl_2}$ and 18C6 in water. The measured heat $Q_i(\mathrm{ex})$ at each injection was corrected for the heat of dilution of the titrant $Q_i(\mathrm{dil})$ to obtain the net heat of the reaction Q_i^{r}.

$$Q_i^{\mathrm{r}} = Q_i(\mathrm{ex}) - Q_i(\mathrm{dil}) \qquad (5)$$

In all calorimetric experiments, 2.7 ml of the ligand solution (4.9 mM CB5/4.5 mM CB7) was taken in a cup and 5 µl of 0.039 M Eu(III) solution in the same medium was injected into the reaction vessel. The heat Q_i^{r} measured at each injection is related to the concentration of complexes formed and their enthalpy of formation (ΔH_n).[29]

$$Q_i^{\mathrm{r}} = -(V_i \sum \beta_n \Delta H_n[\mathrm{M}]_i[\mathrm{L}]_i^n - V_{i-1} \sum \beta_n \Delta H_n[\mathrm{M}]_{i-1}[\mathrm{L}]_{i-1}^n) \qquad (6)$$

where V_i is the volume of the total solution. Nonlinear least square fitting of the Q_i^{r} data was carried out using eqn (6), in conjunction with eqn (3) and (4), to obtain the β_n and ΔH_n values. The first data point (Q_1^{r}) is ignored due to the diffusion of the solution from the capillary to the reaction vessel even before the first injection.

ESI-MS measurements

ESI-MS studies of Eu(III) complexation with CB5 and CB7 in an FAH–water mixture were carried out using a Varian (USA) make instrument (model no. 410) Prostar Binary LC with IT PDA Detectors. Direct infusion masses were collected with a soft ionization technique like ESI (electron spray ionization) in the positive mode using an ion trap.

TRFS measurements

The main aim of TRFS measurements was to obtain information about the primary coordination sphere of the Eu(III) in Eu–CBn complexes which, in turn, provides information about the number of ligand atoms bound to the central metal ion. For this purpose, a TRFS instrument from Jovin Yuon (Sweden) was used. The excitation source is a xenon flash lamp having a frequency of 10 Hz. The excitation wavelength was selected as 396 nm, while the emission spectra were recorded in the wavelength range of 560–640 nm. A monochromatic light from the source falls on the 1 cm thick quartz cell and the fluorescence light emitted at 90° is monitored by an array of diode detectors cooled to −26 °C by the Peltier cooling method. The fluorescence decay spectra were collected in a 2048 channel analyser with a time calibration of 1 µs per channel. The fluorescence decay spectra were fitted into a multi-exponential function to obtain the lifetime of the excited state $^5\mathrm{D}_0$ of Eu(III).

EXAFS measurements

Eu(III) complexes with CB5 and CB7 have been studied with Eu L_3 edge EXAFS to gain some insight into the structure of the complexes. The Eu(III) ion exists in a nine coordinated environment with a regular square antiprismatic geometry.[30] EXAFS measurements have been done on three samples of the following Eu(III) ([Eu]) and CBn ([CBn]) concentrations: (i) [Eu] = 9.0 mM and [CB5] = 16.0 mM, L/M = 1.8, (ii) [Eu] = 9 mM and [CB7] = 34.2 mM, L/M = 3.8 and (iii) [Eu] = 49.4 mM and [CB7] = 18.8 mM, L/M = 0.38. The EXAFS measurements of these samples at the Eu L_3 edge were carried out in the fluorescence mode at the Scanning EXAFS Beamline (BL-9) at the INDUS-2 Synchrotron Source (2.5 GeV, 100 mA) at the Raja Ramanna Centre for Advanced Technology (RRCAT), Indore, India.[31] The beamline uses a double crystal monochromator (DCM) which works in the photon energy range of 4–25 keV with a resolution of $(E/\Delta E) \times 10^4$ at 10 keV. A 1.5 m horizontal pre-mirror with a meridonial cylindrical curvature is used prior to the DCM for the collimation of the beam and a higher harmonic rejection. The second crystal of the DCM is a sagittal cylinder with a radius of curvature in the range 1.28–12.91 meters which provides a horizontal focusing to the beam. For measurements in the fluorescence mode, the sample is placed at 45° to the incident X-ray beam and the fluorescence signal

(I_f) is detected using a Si drift detector placed at 90° to the incident X-ray beam. An ionization chamber detector is used prior to the sample to measure the incident X ray flux (I_0) and a normalized fluorescence of the sample $(\mu = I_f/I_0)$ is obtained as a function of energy by scanning the monochromator over the specified energy range. The EXAFS spectra of the samples at the Eu L_3 edge were recorded in the energy range 6930–7560 eV.

Computational study

Gas phase geometries of CB5, CB7 and their Eu(III) complexes with different coordination geometries are optimized at the GGA level of density functional theory (DFT) by using Becke's exchange functional[32] in conjunction with Perdew's correlation functional[33] (BP86) with generalized gradient approximation (GGA) where 28 electron core pseudopotentials (ECPs) along with the corresponding def-SV(P) basis sets were selected for the Eu(III) ion and all other lighter atoms were treated at the all electron (AE) level.

Results and discussion

UV-Vis spectroscopy

The stability constants $(\log \beta)$ of Eu(III) with CBn were determined by UV-Vis absorption spectroscopy at 25 °C in FAH–water (50 wt%). Fig. 2 gives the spectrophotometric data for CB5 and CB7 titration with Eu(III) in the range λ = 260–340 nm. The experimental and fitted absorbance for CB5 and CB7 titration at λ = 271 and 269 nm, respectively, along with the speciation diagram are given in Fig. 3. The stability constants for Eu–CBn complexes obtained by analyzing spectrophotometric titration data by Hyperquad 2006 are given in Table 1. The UV-Vis spectrophotometric experiments revealed the formation of a 1:1 complex for Eu–CB5 whereas both 1:1 and 1:2 complexes were observed for the Eu–CB7 system.

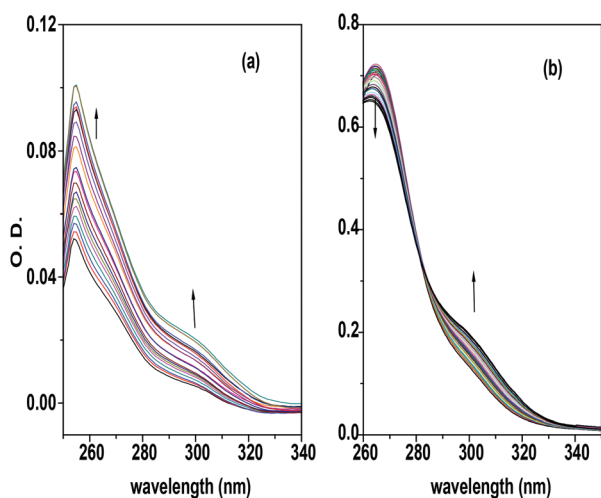**Fig. 2** Spectrophotometric titration of (a) CB5 (1.28×10^{-3} M) and (b) CB7 (9.69×10^{-4}) with Eu(III) in an FA–water mixed solvent at 25 °C.
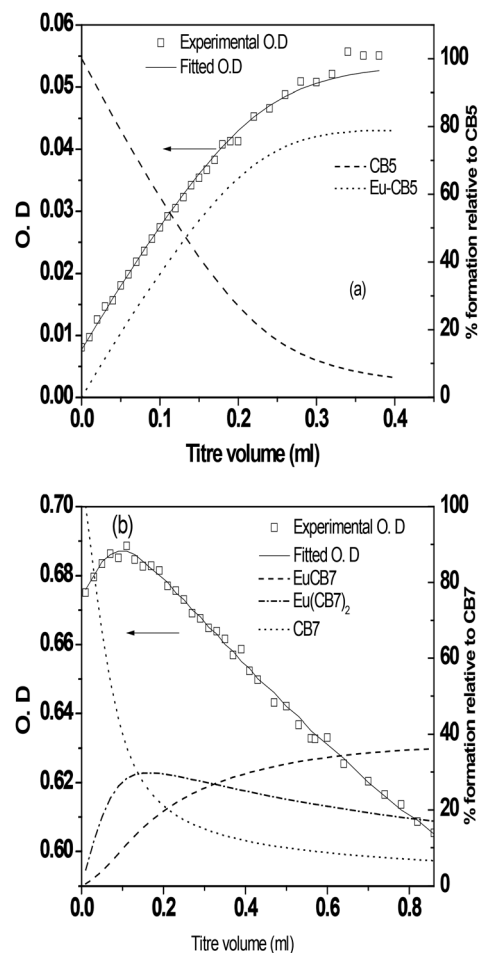

Fig. 3 Plot of absorbance *vs.* titre volume for Eu(III) complexation with (a) CB5 (λ = 271 nm) and (b) CB7 (λ = 269 nm) along with their speciation diagrams.

Table 1 Stability constant for Eu(III) complexes with CB5 and CB7 in an FA–water mixture (50 wt%) at 25 °C

Reaction	Log β	ΔG	ΔH	$T\Delta S$
$Eu^{3+} + CB5 =$ $Eu(CB5)^{3+}$	5.08 ± 0.1 (Calorimetry) 4.78 ± 0.03 (UV-vis)	−28.99	12.1 ± 0.1	41.1
$Eu^{3+} + CB7 =$ $Eu(CB7)^{3+}$	3.45 ± 0.05 (UV-vis)	−19.68	−4.7 ± 0.6	15.0
$Eu^{3+} + 2CB7 =$ $Eu(CB7)_2{}^{3+}$	7.0 ± 0.05 (UV-vis)	−39.94	8.4 ± 0.4	48.3
[a]$Eu^{3+} + CB6 =$ $Eu(CB6)^{3+}$	2.61 ± 0.04 (Calorimetry)	−14.8	−1.7 ± 0.1	13.1

The studies reported on stability constants are carried out either by solubility measurements in an aqueous solution or by calorimetry in an FAH–water mixture.[23,24,34–37] Zhang *et al.* have shown the formation of a 1:1 complex of alkali and alkaline earth metals with CBs *viz.* MeCB5 and CB6 in an FAH–water mixture.[23] The calorimetric studies of CB6 complexation with all the lanthanide ions also reported the formation of a 1:1 complex.[37] Despite the presence of two carbonyl portals in

CB*n*, studies on the metal–CB*n* complexation in solution have shown the binding of a metal ion to only one portal of CB*n*, except for Pb^{2+} and Sr^{2+}.

The basic nature of CB5 is evident from the pK_a value of 9.56[23] while CB6 is weakly acidic (pK_a = 3.02)[38] and in the presence of 50% FAH, the carbonyl portal of CB*n* is expected to be protonated. Zhang *et al.* attributed the competing protonation of CB6 and MeCB5 portals to the binding of the metal ion to only one portal. Only in the case of Pb^{2+}, which has a strong affinity for MeCB5 (log K_1 > 9), the metal ion could also replace a strongly bound proton thus forming a 2 : 1 complex even in an FAH–water mixture.[23] This effect of protonation has also been observed in the Sr–MeCB5 complex (log K = 3.4). Sr–MeCB5 forms a 2 : 1 complex in water whereas a 1 : 1 complex is formed in an FAH–water mixture. Except for Sr^{2+}, the studies on CB*n* complexation with alkali and alkaline earth metals in aqueous solution also reported the formation of only a 1 : 1 complex in the presence as well as the absence of an acid.[34,36] The decrease in charge density in the second portal due to charge polarization, after the binding of Eu(III) in one portal could also be a possible reason for the binding of Eu(III) through only one portal. Contrary to the results in solution, lanthanide ions have been found to form crystalline coordinate polymers where Ln^{3+} binds through both the portals of a CB5 molecule.[10–15,39,40]

The stability constant of Eu(III) with CB*n* of different cavity sizes in solution follows the order CB5 > CB7 > CB6 (Table 1). The charge density on carbonyl oxygen atoms of different CB*n* was found to be nearly the same (described in computational studies). Therefore, the order of stability constant can be explained by the number of carbonyl oxygens interacting with Eu(III). In the case of CB5, the smaller size of the cavity enables Eu(III) to interact with more number of carbonyl oxygen atoms thereby maximizing its interaction with CB5. On the other hand, Eu(III) can bind with only a few of the carbonyl oxygens in the case of CB7 and CB6. The order of stability constant with the cavity sizes reported for MeCB5 and CB6 complexes of alkali and alkaline earth metal ions depends on the ionic size of the metal ion.[36] The stability constant is higher for MeCB5 only in cases where the ionic radii of the metal ions are comparable to the cavity size (K^+ and Sr^{2+}). For cations smaller or bigger than the cavity size (Li^+, Na^+, Rb^+ and Ca^{2+}), CB6 with a larger number of carbonyl oxygen atoms has a higher stability constant than MeCB5.[36] The same trend was also observed in the present work where Eu^{3+} having a radius comparable to the cavity radii of MeCB5 has the highest stability constant. In the absence of a size match between Eu^{3+} and CB*n* (CB6 or CB7), CB7 with a larger cavity size has a higher stability constant than CB6.

The molar absorbance data obtained from Hyperquad 2006, for all the species involved in the titration of CB5 and CB7 with Eu(III) are plotted in Fig. 4. The higher molar absorbance of CB7 compared to CB5 could be the consequence of the presence of more glycoluril groups in CB7. However, the change in the molar absorbance of CB7 on forming a 1 : 1 complex was much less than that for Eu–CB5 (Fig. 4). This larger change in the molar absorbance of the 1 : 1 Eu–CB5
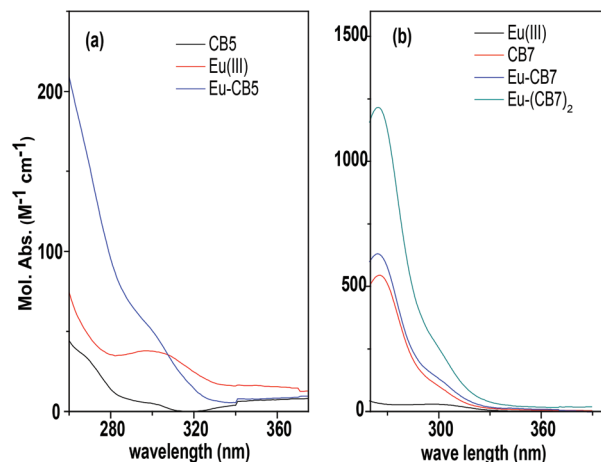

Fig. 4 Molar absorbance spectra of the (a) Eu–CB5 and (b) Eu–CB7 system.

complex compared to the 1 : 1 complex of Eu–CB7 suggests a stronger interaction between Eu(III) and CB5 than with CB7, which is also reflected in the higher stability constant of Eu–CB5.

Calorimetric studies

Fig. 5a and b give the raw calorimetric data (heat flow *vs.* time) for the titration of CB5 and CB7 respectively with Eu(III) in a FAH–water mixture.

The endothermic peaks of complexation and the sharp inflection point at L/M = 1 for Eu–CB5 indicate the formation of a 1 : 1 complex. However, in the case of Eu–CB7, the heat values were endothermic at a low metal concentration (high L/M) and become exothermic at a higher metal concentration (low L/M) which points towards the formation of different species at different L/M ratios (Fig. 6).

In the case of a 1 : 1 complex, the stability constant and ΔH can be calculated by fitting the calorimetric data into eqn (6). However, only calorimetric data cannot give precise ΔH and log β values if more than one species are present. Both log β and ΔH for Eu–CB5 were obtained from the calorimetric data
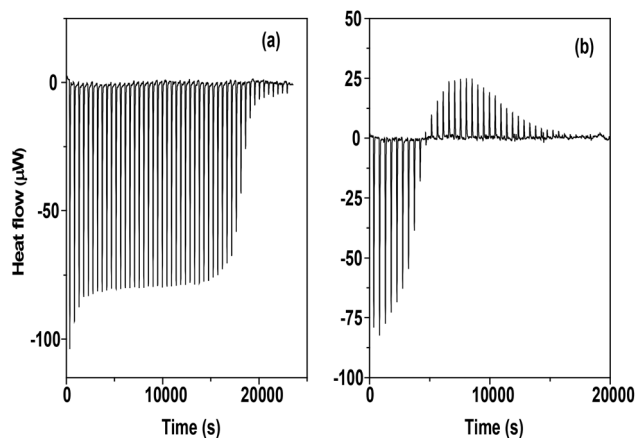

Fig. 5 a and b. Raw calorimetric data (heat flow *vs.* time) for CB5 and CB7 complexation with Eu(III) in an FAH–water mixture at 25 °C.
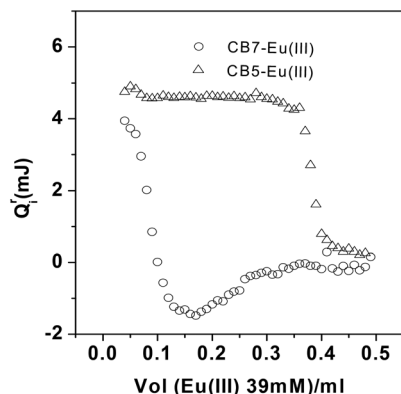
Fig. 6 Plot of heat values at each injection (Q_i^r) on the addition of 10 μl of Eu(III) solution (39 mM).

Fig. 7 Enthalpy and entropy compensation plot for cucurbiturils.

while for Eu–CB7, the stability constant data obtained from spectrophotometric titrations were used to calculate ΔH_1 and ΔH_2 using eqn (6). The thermodynamic data for Eu(III) complexation with CB5 and CB7 are given in Table 1. The stability constant obtained for Eu–CB5 from calorimetry was in good agreement with that obtained from the UV-Vis spectroscopic data. The ΔH of complexation is a result of the enthalpy of bond formation between Eu(III) and carbonyl oxygen, the solvation of the Eu–CBn complex and the enthalpy of desolvation of the metal ion and the CBn molecule. The positive enthalpy of complexation in CB5 suggests that the energy required in desolvation is more than that required in bond formation. This is characteristic of the electrostatic interaction between a hard acid (Eu(III)) and a hard base (CBn) where the metal ion and ligand are strongly hydrated and a large amount of energy is required in desolvation. The entropy of complexation consists of contributions mainly from solvation entropy and conformational entropy. As CBn molecules are rigid and do not undergo significant conformational changes during complexation, ΔS is determined mainly by desolvation of the metal ion and the CBn molecule. Thus, positive ΔS of Eu(III) complexes with CB5 and CB7 indicates an inner sphere complexation wherein solvated water molecules oriented around the metal ion and ligand are released into the bulk solvent and increase the randomness of the system. In spite of more number of carbonyl groups in CB7 compared to CB5, the lower ΔH and ΔS of the 1:1 complexation with Eu(III) indicate the participation of a lesser number of carbonyl groups in the binding of CB7. The comparable value of ΔS for 1:1 Eu–CB5 and 1:2 Eu–CB7 suggests a similar dehydration of Eu(III) in both the cases.

The enthalpy and entropy compensation effect holds for the complexation of cations with a large number of macrocyclic ligands viz., glymes, podands, crown ether, cryptands and macrocyclic antibiotics in various media.[41] However, no such relationship has been reported in the literature for CBn which also belongs to a class of macrocyclic ligands with a unique structure. Thus, it is interesting to find such a correlation for metal CBn complexes. The plot of $T\Delta S$ vs. ΔH for CBn (including present data) is given in Fig. 7.
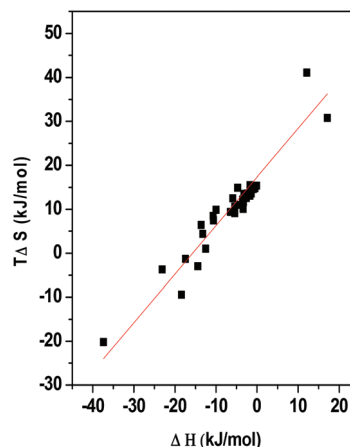
The data used in the plot are taken from ref. 36. The linear relationship between ΔH and $T\Delta S$ suggests that the change in $T\Delta S$ is compensated by a proportional increase in ΔH and vice versa.

$$\Delta(T\Delta S) = \alpha\Delta(\Delta H) \quad (7)$$

$$\text{or } T\Delta S = \alpha\Delta H + T\Delta S_0 \quad (8)$$

where α, the slope of $T\Delta S$ vs. ΔH, is the measure of the cancellation effect and only a $(1 - \alpha)$ fraction of change in ΔH contributes to a change in ΔG. $T\Delta S_0$ is the entropy gain even when ΔH is zero. Though a linear relationship was observed for all macrocyclic ligands, α and $T\Delta S_0$ are reported to be dependent on the type of macrocyclic ligands. The α and $T\Delta S_o$ for different macrocyclic ligands are given in Table 2.

The authors have explained enthalpy and entropy compensation by relating the decrease in ΔH to an increased metal ligand interaction, which is compensated by a decrease in ΔS owing to a simultaneous increase in the rigidity of the ligand structure on complexation.[41]

The α value decreases with an increase in ligand rigidity, that is, glyme/podant > crown ether > cryptand. An increase in the rigidity of the ligand restricts the $T\Delta S$ compensation with ΔH on complexation, thereby decreasing the α value. The same explanation cannot be extended to the rigid macromolecules like antibiotics and CBn which, in spite of their rigid structure have a high α value. In such cases, the enthalpy and entropy compensation can be explained by relating the change in ΔH and ΔS to the dehydration of the metal ion and ligand. Thus, an increase in ΔH due to higher dehydration is compensated

Table 2 Enthalpy–entropy compensation for macrocyclic ligands

Ligand	α	$T\Delta S_0$	Ref.
Glyme	0.86	9.6	41
Crown ether	0.76	10.032	41
Cryptand	0.51	16.72	41
Antibiotic	0.95	23.408	41
CBn	1.1 ± 0.06	17.3 ± 0.7	Present work

by a proportional increase in ΔS due to dehydration entropy. This further supports our assumption of relating ΔS mainly to dehydration entropy. In the case of CBn, the α value and $T\Delta S_0$ were also found to be independent of the cavity size of CBn as can be seen from Fig. 7 which includes data of CB5, CB6 and CB7.

Time resolved fluorescence spectroscopy

The complexation of Eu(III) by CB5 and CB7 was studied by TRFS. The fluorescence spectra and lifetimes were measured as a function of the L/M ratio. Fig. 8 shows the fluorescence spectra normalized with respect to the 592 nm peak at a different L/M ratio. The two prominent fluorescence emission peaks of the Eu(III) ion at 592 nm and 616 nm correspond to transitions $^5D_0-^7F_1$ and $^5D_0-^7F_2$ respectively. $^5D_0-^7F_2$ is a hypersensitive transition due to its electric dipole nature and the intensity ratio of 616 nm and 592 nm (IR) is a measure of the asymmetry of the molecule.[42] The IR was found to increase with L/M due to an increase in the concentration of complexed Eu(III) which is more asymmetric than Eu(H$_2$O)$_9$ (Fig. 9a and b). The sharp increase in IR in the case of CB5 compared to CB7 reflects the stronger binding in the case of CB5–Eu than Eu–CB7. Fig. 10 shows the fluorescence decay profile for

Fig. 10 Fluorescence decay profile of Eu(III) in the presence of CB5 at a ligand to metal (L/M) ratio 0 and 8.0.

Eu–CB5 at L/M = 0 and 8. At all L/M ratio values, the fluorescence was found to follow a monoexponential decay.

A single lifetime can be explained in terms of the fast exchange of metal ions between the free and complexed form which is characteristic of the electrostatic binding and is also observed in Eu(III) complexes with hard donor atoms like in Eu(III) carboxylates.[43] The fluorescence decay lifetime of the excited $^5D_0$ state to the ^7F_i states is quenched by the O–H phonons of water molecules in a non-radiative deexcitation mode. The number of water molecules coordinated to Eu(III) is related to the fluorescence lifetime by the following empirical relationship given by Kimura and Choppin.[44]

$$n_{H_2O} = (1.07/\tau) - 0.62 \qquad (9)$$

In a FAH–water mixture (50 wt%) the Eu(III) lifetime (109 ± 0.5 µs) was found to be the same as that in an aqueous solution (110 µs) which indicates that even in the presence of 50% FAH, FAH molecules are not present in the inner coordination sphere of Eu(III). Fig. 11 gives the τ values with varying L/M ratios for Eu–CB5 and Eu–CB7 and the number of water mole-
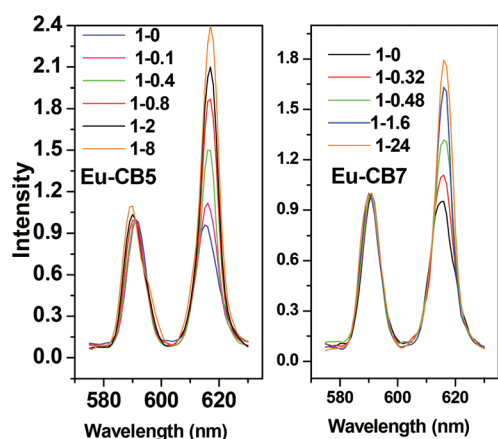

Fig. 8 Fluorescence spectra (normalized with respect to 592 nm) of Eu–CB5 and Eu–CB7 at varying ligand to metal ratios.

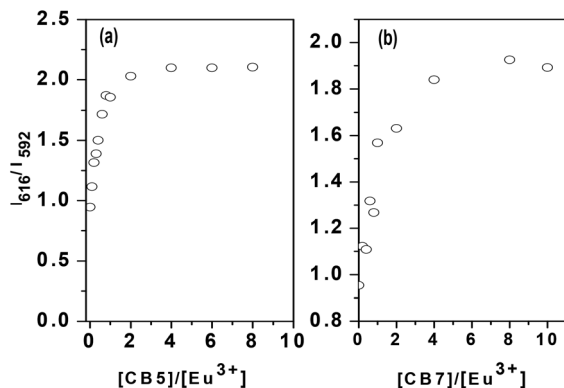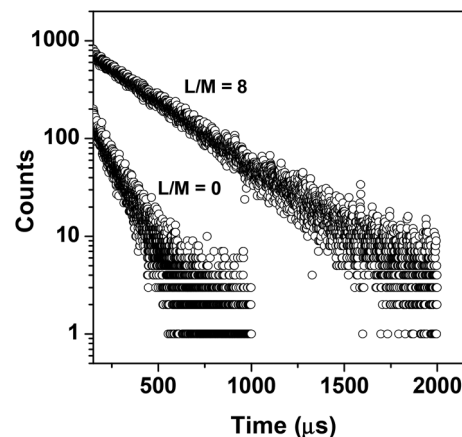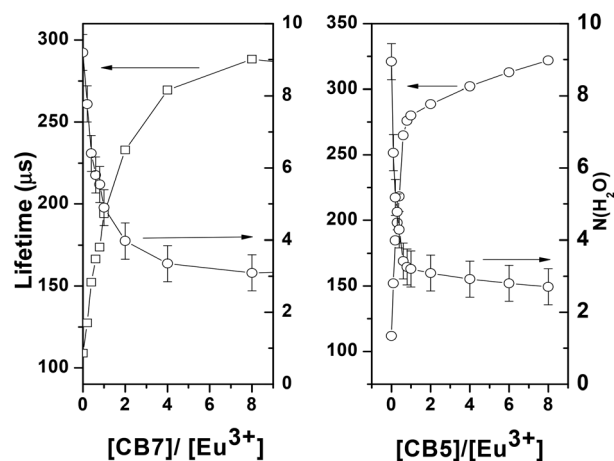Fig. 9 Plot of intensity ratio vs. ligand to metal ratio of CB7 and CB5.

Fig. 11 Plot of fluorescence decay lifetime (τ) and the number of water molecules in the inner coordination sphere of Eu(III).

Table 3 Species identified from ESI-MS spectra of the Eu(III) complexes of CB5 and CB7 at different ligand to metal ratios

Eu–CB5 (L/M = 5)		Eu–CB7 (L/M = 5)		Eu–CB7 (L/M = 1)	
m/z	Species	m/z	Species	m/z	Species
Free ligands		Free ligands		Free ligands	
433.0	$CB5(FAH)_9(H_2O)_3(H^+)_3{}^{3+}$	560.4	$CB7(FAH)_{10}(H_2O)_3(H)_3{}^{3+}$	301.0	$CB7(H)_4(H_2O)_2{}^{4+}$
435.5	$(CB5)(H)_3(FAH)_6(H_2O)_{11}{}^{3+}$	571.4	$CB7(FAH)_{10}(H_2O)_5(H)_3{}^{3+}$	Complex peak	
437.9	$(CB5)(H)_3(FAH)_{10}(H_2O)^{3+}$	Complex peak		578.8	$^{153}Eu(CB7)(FAH)_8(H_2O)^{3+}$
Complex peaks		578.7	$Eu(CB7)(FAH)_8(H_2O)_3{}^{3+}$		
546.8	$Eu(CB5)(FAH)_{10}(H_2O)_{11}{}^{3+}$	561.3	$Eu(CB7)(FAH)_8{}^{3+}$		
		1526.9	$Eu(CB7)_2(FA)(FAH)_{10}(H_2O)_4{}^{2+}$		

cules are calculated using eqn (9) for the corresponding τ values. τ was found to increase with the L/M ratio and saturated at a higher L/M. The increase in τ is due to the removal of water molecules from the inner coordination sphere of Eu(III) during complexation with CBn molecules. The decrease in the number of water molecules further confirms the formation of inner sphere complexes.

According to stability constants, the species present at L/M > 3 (where τ gets saturated) for Eu–CB5 and Eu–CB7 systems are the 1 : 1 and 1 : 2 complexes respectively. The lifetime data suggest the presence of three water molecules in the inner coordination sphere of the 1 : 1 Eu–CB5 complex and 1 : 2 Eu–CB7. The similar entropy values for the formation of 1 : 1 Eu–CB5 and 1 : 2 Eu–CB7 are in agreement with the removal of the same number of water molecules during complexation.

ESI–MS

The ESI-MS measurements were carried out for the Eu–CB5 and Eu–CB7 systems at different ligand to metal ratios. Table 3 gives the details of species identified in the ESI-MS measurements (ESI 1–3†). The most intense peaks in all the spectra correspond to different species of ligands. CB5 was associated with FAH and water molecules to give peaks like $(CB5)$-$(H)_3(FAH)_{10}(H_2O)^{3+}$, $(CB5)(H)_3(FAH)_6(H_2O)_{11}{}^{3+}$, and $CB5$-$(FAH)_9(H_2O)_3(H)_3{}^{3+}$. Only the 1 : 1 complex of Eu(III) with CB5 was observed as $Eu(CB5)(FAH)_{10}(H_2O)_{11}{}^{3+}$ at m/z 546.8, while in the case of the Eu–CB7 spectra at L/M = 5, peaks corresponding to 1 : 1 at m/z 578.7 $(Eu(CB7)(FAH)_8(H_2O)_3{}^{3+})$ and 561.3 $(Eu(CB7)(FAH)_8{}^{3+})$ as well as 1 : 2 complexes at m/z 1526.9 $(Eu(CB7)_2(FA)(FAH)_{10}(H_2O)_4{}^{2+})$ were observed. In the ESI-MS spectra at L/M = 1, the peak corresponding to the 1 : 2 complex was absent whereas that due to the 1 : 1 complex at 578.8 $(^{153}Eu(CB7)(FAH)_8(H_2O)_3{}^{3+})$ was present. The observation in ESI-MS supports the speciation obtained from spectrophotometric as well as calorimetric data. All the species (complexed and uncomplexed) were found to be associated with many FAH and water molecules. Other than the coordinated water molecules of Eu(III), FAH and water molecules solvate the complexed and uncomplexed CBn molecules through hydrogen bonding. A similar solvation of the CB5 complex has been observed in the 2D network of the uranyl-CB5 complex where an environment of nitrate is formed by hydrogen bonding to the carbon bound hydrogen of each CB5 molecule.[12]

EXAFS

Fig. 12 shows the experimental EXAFS ($\mu(E)$ versus E) spectra of the Eu complexes with CBn. In order to take care of the oscillations in the absorption spectra, the energy dependent absorption coefficient $\mu(E)$ has been converted into the absorption function $\chi(E)$ defined as follows:[45]

$$\chi(E) = \frac{\mu(E) - \mu_0(E)}{\Delta\mu_0(E_0)} \tag{10}$$

where E_0 is the absorption edge energy, $\mu_0(E)$ is the bare atom background and $\Delta\mu_0(E_0)$ is the step in the $\mu(E)$ value at the absorption edge. After converting the energy scale to the photoelectron wave number scale (k) as defined by,

$$K = \sqrt{\frac{2m(E - E_0)}{\hbar^2}} \tag{11}$$

the energy dependent absorption coefficient $\chi(E)$ has been converted to the wave number dependent absorption coefficient $\chi(k)$, where m is the electron mass. Finally, $\chi(k)$ is weighted by k^2 to amplify the oscillation at a high k and the functions $\chi(k)\cdot k^2$ are Fourier transformed in the r space to generate the $\chi(r)$ versus r (or FT-EXAFS) spectra in terms of the real distances from the center of the absorbing atom. The Fourier transformed range in the k space is 2–8 Å^{-1}. It should be mentioned here that a set of EXAFS data analysis programs available within the IFEFFIT software package[46] have been used for the reduction and fitting of the experimental EXAFS data. This includes data reduction and Fourier transformation to derive the $\chi(r)$ versus r spectra from the absorption spectra, the generation of the theoretical EXAFS spectra starting from an
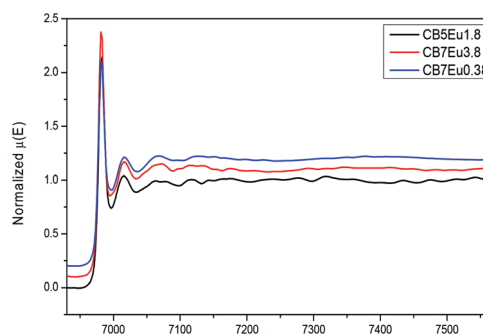

Fig. 12 Plot of absorption coefficient $\mu(E)$ vs. energy.

assumed crystallographic structure and finally fitting of the experimental data with the theoretical spectra using the FEFF 6.0 code. The bond distances, co-ordination numbers (including scattering amplitudes) and disorder (Debye–Waller) factors (σ^2), which give the mean-square fluctuations in the distances, have been used as fitting parameters. The EXAFS measurements for Eu–CB5 were carried out at L/M = 1.8 (labeled as CB5 Eu1.8) where 100% Eu(III) is present as a 1 : 1 complex. In order to deduce the structures of both 1 : 1 and 1 : 2 complexes of Eu–CB7, the EXAFS measurement for CB7 was carried out at two L/M ratios *viz.* 3.8 and 0.38 labeled as CB7 Eu3.8 and CB7 Eu0.38 respectively. According to the speciation diagram obtained from the stability constant, only a 1 : 2 complex of Eu–CB7 is present at L/M = 3.8 and at L/M = 0.38, 35% of Eu is present as a 1 : 1 complex of Eu–CB7 and 65% as free Eu(III).

Fig. 13 shows the experimental plots along with their best fit theoretical plots and the corresponding best fit results for all the samples have been summarized in Table 4. The experimental $\chi(r)$ *versus* r spectra of the CB5 Eu1.8 sample have been fitted from 1.4 to 3.5 Å with two Eu–O shells at 2.22 Å (n = 3.0) (Eu–O1) and 2.98 Å (n = 6.5) (Eu–O2) and an Eu–C shell at 3.56 Å (n = 6.6). The presence of an Eu–C shell is an indicator of the binding of Eu(III) through the carbonyl oxygen of CB5 or formate and the same number of oxygen should correspond to carbonyl oxygen or formate oxygen (Eu–O2). The Eu–O1 shell therefore can be assigned to the oxygen atoms of the co-ordinated water molecule. The higher N (6.5 ± 0.7) of Eu–O2 shell cannot be explained by binding through CB5 as it can donate a maximum of five oxygen atoms. The binding of formate encapsulated inside the cavity to Eu(III) could possibly

be the reason for a higher number of Eu–O2 and Eu–C bonds. Though no evidence for anion encapsulation has been furnished in the present work, the encapsulation of anions *viz.*, nitrate and chloride, in a CB5 solution has been shown by fluorescence studies.[39] The higher affinity of the nitrate ion for CB5 compared to the chloride ion has been attributed to its more diffused negative charge. Thus, a diffused negative charge on formate and a high concentration of formic acid (11.11 m) in the medium collectively support the possibility of formate encapsulation. The encapsulation of chloride and nitrate has also been observed in crystal studies.[39,40] In a 1 : 1 Eu–CB5 complex, Eu(III) is symmetrically bound to CB5, covering one of the two portals. A number of literature reports on the crystal structure of lanthanide–CB5 have shown the binding of lanthanide ions in different coordination modes depending on the crystallization conditions or cation size. Studies by K. Chen on crystalline Eu–CB5 have shown the binding of Eu(III) to one CB5 molecule in two different modes.[47] One Eu(III) fully capped the portal by binding symmetrically to all the carbonyl oxygen while the second Eu(III) bound partially to another portal of the same CB*n* molecule. The Eu–O distance reported for the fully capped portal is in the range 2.806–2.959 Å and for the partially capped is 2.900–3.290 Å which is close to that obtained in the present work for 1 : 1 Eu–CB5. The CB7 Eu0.38 spectrum for the 1 : 1 Eu–CB7 species has been fitted with two Eu–O shells at 2.35 Å (n = 6.0) and 3.03 Å (n = 2.9). The EXAFS results on CB7 Eu0.38 indicate the binding of Eu(III) to only three oxygen atoms from the carbonyl oxygen atoms of CB7 and formate oxygen and the remaining coordination is satisfied by six water molecules. This asymmetric binding of CB7 can be attributed to the small size of Eu(III).

The symmetric binding of Eu(III) by CB5 is also evident from a higher $\log \beta$ of Eu–CB5 compared to Eu–CB7 which is mainly due to a higher ΔS in Eu–CB5. The higher ΔS of Eu–CB5 can be explained by the removal of six coordinated water molecules of Eu(III) compared to that in Eu–CB7 where only three water molecules are removed. The loss of more number of hydrated water molecules by Eu(III) upon complexation with CB5 is also reflected in its higher ΔH in contrast to exothermic ΔH for 1 : 1 Eu–CB7. The ΔH reported for CB6 (−1.7 ± 0.1 kJ mol^{-1}) [37] is also similar to that obtained for Eu–CB7 (−4.7 ± 0.6 kJ mol^{-1}). The higher dehydration of Eu(III) therefore can be attributed to its interaction with more number of carbonyl oxygens.

Eu(III) in CB5 is encapsulated through one portal and has only three residual water molecules and their removal by one
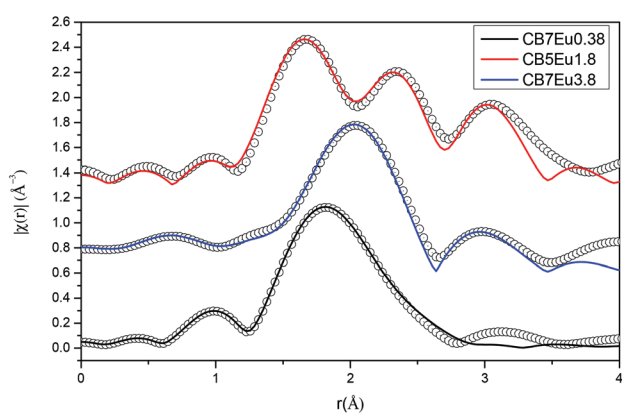

Fig. 13 Plot of $\chi(r)$ vs. r.

Table 4 Fitting Results of Eu L$_3$ edge EXAFS spectra Eu−CB*n* complexes

	CB5 Eu1.8			CB7 Eu3.8			CB7 Eu0.38		
	r (Å)	N	σ^2	r (Å)	N	σ^2	r (Å)	N	σ^2
Eu–O1	2.22 ± 0.01	3.0 ± 0.4	0.0015 ± 0.002	2.51 ± 0.01	8.9 ± 1.1	0.017 ± 0.003	2.35 ± 0.04	6.0 ± 0.2	0.011 ± 0.001
Eu–O2	2.98 ± 0.01	6.5 ± 0.7	0.001 ± 0.001	—	—	—	3.03 ± 0.09	2.9 ± 0.6	0.011 ± 0.006
Eu–C	3.56 ± 0.02	6.6 ± 0.8	0.001 ± 0.004	3.44 ± 0.03	5.8 ± 2.1	0.001 ± 0.004	—	—	—

more CB5 molecule could be geometrically more unfavorable. Unlike in Eu–CB5, Eu(III) in the 1:1 Eu–CB7 complex has six water molecules, therefore, the three residual water molecules can be easily replaced by another CB7 molecule, thus forming a 1:2 complex. The EXAFS data of CB7 Eu3.8, where the presence of only 1:2 Eu–CB7 is expected, have been fitted with an Eu–O shell at 2.51 Å ($n = 9.0$) and an Eu–C shell at 3.44 Å ($n = 5.8$). The presence of nearly six carbon atoms at 3.44 Å suggests that nearly six oxygen atoms at a distance of 2.51 Å are from the carbonyl group of the two CB7 molecules and the rest three are from the coordinated water molecules. The binding of one metal ion to two CB7 molecules to give one dimensional polymer is very common in crystal studies.[17] For a simple hard acid and hard base reaction, where electrostatic interactions play a dominant role, the affinity of the metal ion for successive ligands decreases due to the neutralization of the charge on the metal ion and the stability constant follows the order $\log K_1 > \log K_2$. But, in the case of Eu–CB7, $\log K_2$ (3.55 ± 0.05) was found to be nearly the same as $\log K_1$ (3.45 ± 0.05). The extra stability of the 1:2 Eu–CB7 complex can be attributed to the closer approach of Eu(III) to the two CB7 molecules which can be seen from the shorter Eu(III) and carbonyl oxygen distances in EXAFS results for CB7 Eu3.8 than those in 1:1 Eu–CB7 (Table 4). Kitano *et al.* have empirically related the ΔS of complexation to the number of released water molecules.[48] A similar ΔS for 1:1 Eu–CB5 and 1:2 Eu–CB7 complexes indicates the removal of nearly the same number of water molecules from the inner coordination sphere of Eu(III). In both complexes, 1:1 Eu–CB5 and 1:2 Eu–CB7, the inner coordination sphere of Eu(III) is associated with three water molecules at a distance 2.98 ± 0.01 Å and 2.51 ± 0.01 Å respectively, which is in line with the fluorescence lifetime studies and similar ΔS values for the formation of Eu–CB5 and Eu(CB7)$_2$. Eu(III) in all the three species 1:1 Eu–CB5, 1:1 Eu–CB7 and 1:2 Eu–CB7, is found to bind in different mode. The results of all the three EXAFS measurements have shown a shorter Eu–O (H$_2$O) compared to Eu–O(>C=O) as also reported in some of the crystal studies.[47] The rigid structure of

CBn molecules restricts the oxygen atoms to come close to Eu(III) whereas water molecules can easily approach closer to Eu(III).

Computational studies

CB5 *vs.* CB7. The optimized structure of CB5 and CB7 is given in Fig. 1. The radius of the incircle (R_i) of the pentagon formed by joining five portal oxygens of CB5, calculated from the average bond distance between carbonyl oxygens in optimized geometry, was found to be 2.31 Å (described in ESI 4†). Similarly, R_i calculated for CB7 was found to be 3.95 Å. The natural charges on carbonyl oxygens of CB5 ($0.577e^-$) were found to be nearly the same as those on CB7 ($0.585e^-$). Therefore, the stability of a complex should depend on the number of carbonyl oxygen atoms interacting with Eu(III) and their distance.

Eu–CB5. DFT calculations of CB5 and its complexes with Eu(III) were carried out to determine their most stable geometries and the natural charges on binding atoms. The optimized structure of CB5 and Eu–CB5 along with the natural charge on oxygen and Eu are given in Fig. 14. Eu(III) was found to bind symmetrically with all the five carbonyl oxygen atoms at an average distance of 2.47 Å and the complexation of Eu(III) led to the constriction of the CB5 portal (bound to Eu(III)), that is, R_i of the portal decreased from 2.31 to 1.92 Å. Interestingly, the R_i of the nonbonding portal also decreased to 2.18 Å. The crystal structural studies on Eu(III) complexes with CB5 showed an enlargement of the other portal which leads to an asymmetric binding of the second Eu(III) to give one dimensional polymers. The symmetric binding of Eu(III) with all the carbonyl oxygens supports the Eu(III) coordination observed in the present work. The binding energy of Eu(III) with CB5 in the gas phase was found to be ($\Delta E = E_{\text{Eu–CB5}} - E_{\text{CB5}} - E_{\text{Eu}^{3+}}$, E_x is energy of species 'X') – 26.04 eV. The natural charge on Eu(III) decreased from +3e^- to +1.847e^- and the charges on carbonyl oxygens bound to Eu(III) increased from $-0.577e^-$ (in free CB5) to $-0.734e^-$. The increase in the charge on carbonyl oxygen atoms (bound to Eu(III)) on binding with Eu(III) is due to the
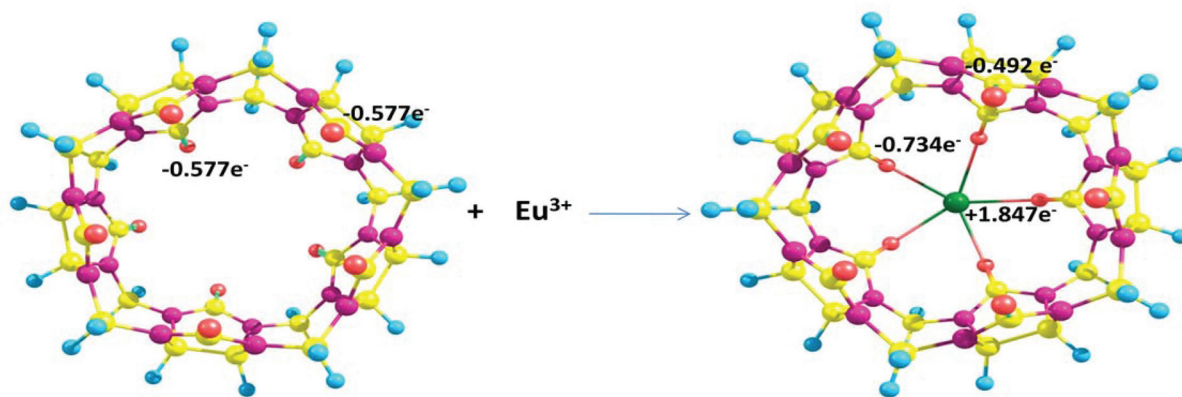

Fig. 14 Optimized structure of CB5 and Eu–CB5 and natural charges on Eu(III) and carbonyl oxygen atoms, obtained from DFT calculations (europium atom (green), Oxygen atom (red), Hydrogen atom (blue), Nitrogen atom (purple) and Carbon atom (yellow)).

charge polarization from the non bonding carbonyl oxygen atoms of another portal. Charge polarization can also be observed from a decrease in the natural charges on oxygen atoms of the non-bonding portal (Fig. 14). The reduction in R_i at the non-bonding portal is due to the reduced electrostatic repulsion on oxygen atoms. The charge polarization in CB5 on binding with Eu(III) reduces the affinity of the second portal for Eu(III), and could be one of the reasons that a 2 : 1 complex is not formed.

In order to understand the role of hydrated water molecules in complexes and their geometry, the structures of Eu–CB5 were also optimized with three water molecules coordinated to Eu(III) in two different geometries (i) one water molecule co-ordinated from inside the cavity and two water molecules from outside (Eu–CB5 A); (ii) all the three water molecules are co-ordinated from outside (Eu–CB5 B) (ESI 5†). Interestingly, in the Eu–CB5 B geometry, Eu(III) was found to bind only four oxygen atoms directly and the fifth oxygen was bound through coordinated water molecules. On the other hand, in the Eu–CB5 A geometry, all the carbonyl oxygens were bound directly to Eu(III). The interaction of Eu(III) with the five carbonyl oxygen atoms in Eu–CB5 A leads to a higher charge neutraliz-ation of Eu(III) (+3 to $1.612e^-$) compared to that in Eu–CB5 B (+3 to $+1.655e^-$) (ESI 5†) whereas ΔE was found to be compar-able for both the geometries.

The studies described in the above sections point towards the binding of Eu(III) with all the five carbonyl oxygen atoms of CB5, a formate and three water molecules. In order to find the possibility of the formation of the proposed species with formate encapsulation, Eu–CB5(H$_2$O)$_3$(FA), where FA is en-capsulated inside the cavity, the geometry for the same was opti-mized to get a minimum energy structure (Fig. 15). The energy for the formation of Eu–CB5(H$_2$O)$_3$(FA) ($\Delta E = E_{\text{Eu–CB5(H}_2\text{O)}_3\text{(FA)}} - E_{\text{Eu}^{3+}} - E_{\text{CB5}} - E_{\text{FA}} - E_{\text{H}_2\text{O}}$) was found to be -40.294 eV. ΔE for the formation of Eu–CB5(H$_2$O)$_3$(FA) was most negative com-pared to all the possible species studied in the present work (Table 5). The high stabilization of the structure on the encap-sulation of formate in the CB5 cavity suggests the important role of anion encapsulation in determining the stability of the complex. Eu(III) in the optimized geometry was found to inter-act directly with all the carbonyl oxygens but a small asymme-try was introduced by the presence of formate in the cavity. The Eu–O (>C=O) bond distance of the bound portal varied in the range 2.49 to 2.64 Å and the charges on the oxygen atoms also varied in the range -0.672 to $-0.701e^-$. The average Eu–O bond distance in the presence of an encapsulated formate increased from 2.51 (in Eu–CB5 A) to 2.58 Å which can be attributed to the decrease in the charge density on the Eu atom and an increased coordination number. The reduction of the natural charge on Eu(III) from +3 to $+1.497e^-$ is expected to reduce its affinity for another CB5 molecule and thereby reduces the possibility of the formation of a 1 : 2 complex.

Eu–CB7. In the optimized structure of the Eu–CB7 complex (in the absence of water and formate), Eu(III) was found to interact with only three carbonyl oxygens with an interaction energy of -25.544 eV. Similar to Eu–CB5, a charge polarization
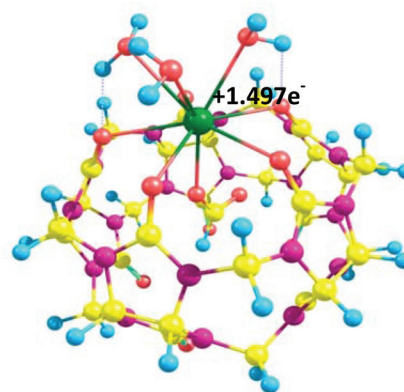

Fig. 15 Optimised structure of Eu(CB5)(FA)(H$_2$O)$_3$ (europium atom (green), Oxygen atom (red), Hydrogen atom (blue), Nitrogen atom (purple) and Carbon atom (yellow)).

Table 5 Theoretically calculated binding energies of complexes

Species	ΔE (eV)	Natural Charge on 'Eu'
Eu CB5	-26.041	$+1.847$
Eu(CB5)(H$_2$O)$_3$, Eu–CB5 B Eu-CB5 B	-29.974	$+1.655$
Eu(CB5)(H$_2$O)$_3$, Eu–CB5 A Eu-CB5 A	-29.828	$+1.612$
Eu(CB5)(H$_2$O)$_3$(FA)	-40.294	$+1.497$
Eu CB7	-25.544	$+1.791$

was also observed in the Eu–CB7 complex. The charges on oxygen atoms of CB7 that are bound to Eu(III) increased from $-0.585e^-$ to nearly $0.8e^-$ whereas the charges on non-bonding oxygen atoms on the same portal decreased slightly (from $-0.585e^-$ to nearly $-0.533e^-$). The unsymmetrical binding of Eu(III) with three carbonyl oxygen atoms supports the thermo-dynamic and spectroscopic results. The smaller ΔE and lesser charge neutralization of Eu(III) on complexation with CB7 com-pared to CB5 (Table 5) is in line with the lower stability con-stant of Eu–CB7 (Table 1). The spectroscopic studies on the 1 : 1 Eu–CB7 complex point towards the presence of six Eu–O bonds from water molecules and three Eu–O bonds from the carbonyl oxygen of CB7 and formate. The geometry of the 1 : 1 Eu–CB7 complex was optimized with Eu(III) bound to six water molecules and one CB7 molecule (Eu(CB7)(H$_2$O)$_6$). However, the minimum energy geometry obtained for the species Eu(CB7)(H$_2$O)$_6$ showed the binding of Eu(III) to the portal of the CB7 molecule by hydrogen bonding through coordinated water molecules around Eu(III) (Fig. 16). Such outer sphere complexes have been reported in the literature for Yb(H$_2$O)$_8$$^{3+}$ and CB7.[49] Though there are many reports on the presence of outer sphere complexes of metal ions with CBn,[13,14] the opti-mized geometries obtained were in contrast to experimental observations where Eu(III) forms an inner sphere complex with CB7. The geometry for 1 : 1 Eu–CB7 with encapsulated formate and water molecules (Eu(FA)CB7(H$_2$O)$_6$) could not be con-verged in the same level of calculation.
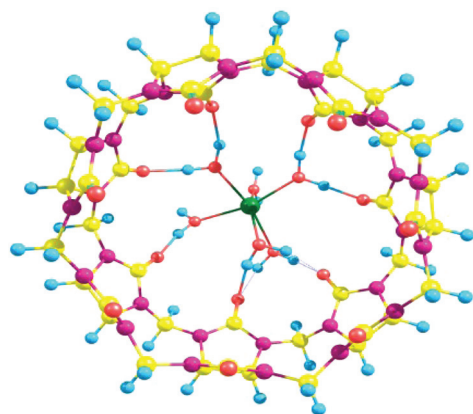
Fig. 16 Optimised structure of Eu(CB7)(H$_2$O)$_6$ (europium atom (green), Oxygen atom (red), Hydrogen atom (blue), Nitrogen atom (purple) and Carbon atom (yellow)).

Conclusions

The present study has shown the role of the cavity size of CBn on the stoichiometry, stability constant and structure of Eu(III) complexes with CB5 and CB7. Thermodynamic studies on Eu–CBn complexation revealed the formation of a 1:1 complex with CB5 while 1:1 and 1:2 complexes were observed with CB7 which has also been corroborated by ESI-MS studies. The complexation reactions have been found to be driven by entropy which is attributed to the dehydration of Eu(III) and CBn during complexation. Both EXAFS and TRFS have shown the presence of three water molecules in the inner coordination sphere of Eu(III) in the 1:1 Eu–CB5 and 1:2 Eu–CB7 complexes which are in line with their ΔS values. Thermodynamic, TRFS and EXAFS studies have shown the symmetric binding of Eu(III) with all the five carbonyl oxygens in the 1:1 Eu–CB5 complex whereas only a few of the CB7 carbonyl oxygens were present in the first coordination shell of Eu(III) in the 1:1 complex of Eu–CB7. In the case of 1:2 complex of Eu–CB7, six carbonyl oxygens are present which illustrates that Eu(III) is sandwiched between two CB7 molecules each coordinating through three carbonyl oxygens. These observations have also been supported by DFT calculations on Eu–CBn complexes.

Acknowledgements

Notes and references

1 E. Masson, X. Ling, R. Joseph, L. Keyeremeh-Mensah and X. Lu, *RSC Adv.*, 2012, **2**, 1213.

2 Y. Chen and Y. Liu, *Chem. Soc. Rev.*, 2010, **39**, 495; R. Ludwig and N. T. Kim Dzung, *Sensors*, 2002, **2**, 397.

3 C. Márquez, R. R. Hudgins and M. N. Werner, *J. Am. Chem. Soc.*, 2004, **126**, 5806.

4 M. R. Craig, M. G. Hutchings, T. D. W. Claridge and H. L. Anderson, *Angew. Chem., Int. Ed.*, 2001, **40**, 1071.

5 J. W. Steed and J. L. Atwood, *Supramolecular Chemistry*, Wiley Publication, 2nd edn, 2009.

6 K. Moon and A. E. Kaifer, *Org. Lett.*, 2004, **6**, 185.

7 W. L. Mock and N. –Y. Shih, *J. Org. Chem.*, 1986, **51**, 4440.

8 H. –J. Buschmann, A. Wego, A. Zielesny and E. Schollmeyer, *J. Inclusion Phenom. Macrocyclic Chem.*, 2006, **54**, 241.

9 M. V. Rekharsky, T. Mori, C. Yang, Y. H. Ko, N. Selvapalam, H. Kim, D. Sobransingh, S. Kaifer Lui, L. Isaacs, W. Chen, S. Moghaddam, M. K. Gilson, K. Kim and Y. Inoue, *Proc. Natl. Acad. Sci. U. S. A.*, 2007, **104**, 20737.

10 S. Khushwaha, S. Rao, A. Padamraja and P. Sudhakar, *Inorg. Chem.*, 2012, **51**, 267.

11 Y.-M. Jeon, J. Kim, D. Whang and K. Kim, *J. Am. Chem. Soc.*, 1996, **118I**, 9790.

12 J. Heo, J. Kim, D. Whang and K. Kim, *Inorg. Chim. Acta*, 2000, **297**, 307.

13 X. Feng, X.-J. Lu, S.-F. Xue, Y.-Q. Zhang, Z. Tao and Q.-J. Zhu, *Inorg. Chem. Commun.*, 2009, **12**, 849.

14 D. G. Samsonenko, M. N. Sokolov, A. V. Virovets, N. V. Pervukhina and V. P. Fedin, *Eur. J. Inorg. Chem.*, 2001, 167.

15 E. A. Mainicheva, O. A. Gerasko, L. A. Sheludyakova, D. Yu. Naumov, M. I. Naumova and V. P. Fedin, *Russ. Chem. Bull.*, 2006, **55**, 267.

16 P. Thuèry, *Inorg. Chem.*, 2010, **49**, 9078.

17 P. Thuèry and B. Masci, *Cryst. Growth Des.*, 2010, **10**, 716.

18 P. Thuèry, *Cryst. Growth Des.*, 2011, **11**, 2606.

19 P. Thuèry, *Inorg. Chem.*, 2011, **50**, 10558.

20 W. A. Freeman, W. L. Mock and N. Y. Shih, *J. Am. Chem. Soc.*, 1981, **103**, 7367.

21 W. L. Mock and N. Y. Shih, *J. Org. Chem.*, 1986, **51**, 4440.

22 W. L. Mock and N. Y. Shih, *J. Am. Chem. Soc.*, 1989, **111**, 2697.

23 X. X. Zhang, K. E. Krakowiak, X. Xue Guoping, J. S. Bradshaw and R. M. Izatt, *Ind. Eng. Chem. Res.*, 2000, **39**, 3516.

24 H.-J. Buschmann, K. Jansen and E. Schollmeyer, *Inorg. Chem. Commun.*, 2003, **6**, 531.

25 R. Ruhela, B. S. Tomar, A. K. Singh, R. C. Hubli and A. K. Suri, *Dalton Trans.*, 2013, **42**, 7085.

26 J. Kim, I.-S. Jung, S. –Y. Kim, E. Lee, J. -K. Kang, S. Sakamoto, Y. Kentaro and K. Kim, *J. Am. Chem. Soc.*, 2000, **122**, 540.

27 P. Gans, A. Sabatini and A. Vacca, *Talanta*, 1996, **43**, 1739.

28 P. Johansson and I. Wadso, *Thermochim. Acta*, 1999, **342**, 19.

29 N. Rawat, R. B. Gujar, M. S. Murali, B. S. Tomar and V. K. Manchanda, *Thermochim. Acta*, 2009, **488**, 21.

30 L. Helm, F. Foglia, T. Kowall and A. E. Merbach, *J. Phys.: Condens. Matter*, 1994, **6 A**, 137.

31 S. Basu, C. Nayak, A. K. Yadav, A. Agrawal, A. K. Poswal, D. Bhattacharyya, S. N. Jha and N. K. Sahoo, *J. Phys.: Conf. Ser.*, 2014, **493**, 12032.

32 A. D. Becke, *Phys. Rev. A*, 1988, **38**, 3098.

33 J. P. Perdew, *Phys. Rev. B: Condens. Matter*, 1986, **33**, 8822.

34 H. J. Buschmann, E. Cleve, L. Mutihac and E. Schollmeyer, *J. Inclusion Phenom. Macrocyclic Chem.*, 2009, **65**, 293.

35 X. X. Zhang, K. E. Krakowiak, G. Xue, J. S. Bradshaw and R. M. Izatt, *Ind. Eng. Chem. Res.*, 2000, **39**, 3516.

36 H. J. Buschmann, K. Jansen, C. Meschke and E. Schollmeyer, *J. Solution Chem.*, 1998, **27**(2), 135.

37 H. –J. Buschmann, K. Jansen and E. Schollmeyer, *Inorg. Chem. Commun.*, 2003, **6**, 531.

38 H. –J. Buschmann, E. Cleve and E. Schollmeyer, *Inorg. Chim. Acta*, 1992, **93**, 193.

39 J. –X. Liu, L.- S. Long, R. B. Huang and L. S. Zhen, *Inorg. Chem.*, 2007, **46**, 10168.

40 J. –X. Liu, L.- S. Long, R. B. Huang and L. S. Zhen, *Cryst. Growth Des.*, 2006, **6**, 2611.

41 Y. Inoue and T. Hakushi, *J. Chem. Soc., Perkin Trans. 2*, 1985, 935.

42 G. Blasse and B. C. Grabmaier, *Luminescent Material* , Springer Verlag, 1994.

43 N. Rawat, A. Bhattacharyya, B. S. Tomar, T. K. Ghanty and V. K. Manchanda, *Thermochim. Acta*, 2011, **518**, 111.

44 T. Kimura and G. R. Choppin, *J. Alloys Compd.*, 1994, **231/214**, 313.

45 D. C. Konigsberger and R. Prince, *X-Ray Absorption: Principles, Applications, Techniques of EXAFS, SEXAFS and XANES*, Wiley, New York, 1988.

46 M. Newville, B. Ravel, D. Haskel, J. J. Rehr, E. A. Stern and Y. Yacoby, *Physica B*, 1995, **208/209**, 154.

47 K. Chen, L. L. Liang, H. J. Liu, Y. Q. Zhang, S. F. Xue, Z. Tao, X. Xiao, Q. J. Zhu, L. F. Lindoy and G. Wei, *CrystEngComm*, 2012, **14**, 7994.

48 H. Kitano, Y. Onishi, A. Kirishima, N. Sato and O. Tochiyama, *Radiochim. Acta*, 2006, **94**, 541.

49 P. Thuèry, *Inorg. Chem.*, 2009, **48**, 4497.